2.1 INTRODUCTION

Vitiligo is a multifactorial, depigmenting skin disorder characterized by loss of functional melanocytes (Ortonne and Bose, 1993). Precise etiology of vitiligo is still unknown. It is a polygenic disorder involving both multiple susceptibility genes (Majumder *et al*., 1993; Nath *et al*., 1994; Sun *et al*., 2006), perhaps in different combinations in different populations, and unknown environmental triggers. Vitiligo is accompanied by oxidative stress characterized by overproduction and accumulation of H_2O_2. Oxidative stress is considered to be the initial pathogenic event in melanocyte destruction (Schallreuter *et al*., 1991; Maresca *et al*., 1997; Laddha *et al*., 2013). Oxidative stress can occur due to an increased concentration of ROS and/or a reduction in antioxidant capacity. There are three major antioxidant enzymes responsible for maintaining the intracellular oxidative homeostasis and they include superoxide dismutases (SODs), glutathione peroxidase (GPX) and catalase enzymes. GPX is a selenoenzyme that catalyses the breakdown of H_2O_2 and other organic peroxides into H_2O and O_2 and the corresponding alcohols using reduced glutathione (GSH) as an essential co-substrate. Seven isoforms of GPX have been identified in humans (Rotruck *et al*., 1973; Zotova *et al*., 2004; Hamanishi *et al*., 2004; El-Far *et al*., 2005; Papp *et al*., 2007). GPX1 is a major intracellular antioxidant enzyme of all cell types (Zotova *et al*., 2004; Handy *et al*., 2009). Various researchers have demonstrated decreased GPX activity in lesional and non-lesional epidermal skin (Hasse *et al*., 2004), PBMCs (Zailaie *et al*., 2005), whole blood (Beazley *et al*., 1999; Jalel *et al*., 2009), erythrocytes (Yildirim *et al*., 2003; Ines *et al*., 2006) and significant increase in erythrocyte LPO levels from vitiligo patients (Picardo *et al*., 1994; Yildirim *et al*., 2003; Agrawal *et al*., 2004; Koca *et al*., 2004; Shajil and Begum, 2006; Ines *et al*., 2006; Shajil *et al*., 2007). *GPX1* Leu200Pro (rs1050450) SNP has been extensively reported in several diseases like cancer (Ratnasinghe *et al*., 2000; Chen *et al*., 2011), type 2 diabetes (Hamanishi *et al*., 2004), Keshan disease (Wei *et al*., 2011), wherein it was reported to decrease GPX1 activity (Hu and Diamond, 2003). However, in our previous study this SNP was found to be uninformative in vitiligo patients (Shajil *et al*., 2007). Therefore, we hypothesized that other polymorphism/s might be responsible for the decreased GPX1 activity in vitiligo.

In the present study, SNPs were selected based on bioinformatics analysis. We performed sequence based analysis to predict the impact of *GPX1* exon1 G/C (rs8179169; Arg5Pro), T/C (rs4991448; Leu6Pro); exon2 C/T (rs6446261; Ala194Thr) polymorphisms on GPX1 protein using *in silico* prediction tools. Our results revealed decreased stability of Leu6Pro and Ala194Thr variants compared to native structure, which will in turn affect the function of the protein and Arg5Pro, Leu6Pro variants show disease like trait. Therefore, the present study was aimed to investigate: i) *GPX1* Arg5Pro, Leu6Pro, Ala194Thr polymorphisms, ii) to estimate erythrocyte GPX1 activity and LPO levels, iii) to estimate *GPX1* transcript levels in PBMCs from vitiligo patients and controls from Gujarat population, and iv) to analyze the structural and functional impacts of these variations on GPX1 protein using *in silico* tools.

2.2 MATERIALS AND METHODS

2.2.1 Study Subjects:

The study group included 521 vitiligo patients where 387 patients were having generalized vitiligo (including acrofacial vitiligo and vitiligo universalis) and 134 were with localized vitiligo; 380 patients were with active vitiligo and 141 with stable vitiligo; comprised of 235 males and 286 females who referred to S.S.G. Hospital, Vadodara, Gujarat, India (Table 1). Inclusion criteria followed for recruitment of patients were: outpatients of sex, age between 5 to 60 years, with generalized or localized vitiligo and both the parents should be Gujarati by birth. We used the following clinical criteria to define the stability proposed by Falabella *et al*. (1995), and discussed in the Vitiligo Global Issues Consensus Conference, 2012 (Ezzedine *et al*., 2012): (i) lack of progression of old lesions within the past 2 years; (ii) no new lesions developing within the same period. Active disease was defined as, appearance of new lesions and spreading of existing lesions observed during past two year duration. The diagnosis of vitiligo was clinically based on the presence of depigmented patches on the skin. A total of 614 ethnically sex-matched unaffected controls (272 males and 342 females) were included in the study (Table 1). Inclusion criteria followed for recruitment of controls were: age between 5 to 60 years, individuals must be unrelated; individuals who are willing to participate in the study and both the parents should be Gujarati by birth. Individuals having any evidence of vitiligo and/or family history, individuals with apparent health problems e.g. hepatic disorders, etc., individuals who were previously enrolled in this trial, individuals who are unwilling to participate in the study were excluded. The mean age (years ± SD) of patients and healthy controls were 31.21 ± 11.45 and 28.41 ± 12.16 respectively (Table 1). The study plan was approved by the Institutional Ethical Committee for Human Research (IECHR), Faculty of Science, The Maharaja Sayajirao University of Baroda, Vadodara, Gujarat, India. The importance of the study was explained to all participants and written consent was obtained from all patients and controls.

2.2.2 Genomic DNA Preparation:

Five ml venous blood was collected from the patients and healthy subjects in K_3EDTA coated vacutainers (BD, Franklin Lakes, USA). Genomic DNA was extracted from whole blood using QIAamp DNA Blood Kit (QIAGEN Inc., Valencia, USA) according to the manufacturer's instructions. After extraction, concentration and purity of DNA was estimated spectrophotometrically, quality of DNA was also determined on 0.8% agarose gel electrophoresis and DNA was stored at -20^{o}C until further analyses.

Table 1. Demographic characteristics of Gujarat vitiligo patients and controls.

Particulars	Vitiligo Patients	Controls
	(n = 521)	(n = 614)
Average age (mean age ± SD)	31.21 ± 11.45 yr	28.41 ± 12.16 yr
Sex: Male	235 (45.11%)	272 (44.30%)
Female	286 (54.89%)	342 (55.70%)
Age of onset (mean age ± SD)	21.86 ± 12.83 yr	NA
Duration of disease (mean ± SD)	8.12 ± 7.34 yr	NA
Type of vitiligo		
Generalized vitiligo	387 (74.23%)	NA
Localized vitiligo	134 (25.73%)	NA
Active vitiligo	380 (72.86%)	NA
Stable vitiligo	141 (27.14%)	NA

Table 2. Primers and restriction enzymes used for genotyping of *GPX1* exon 1 G/C (rs8179169); exon 1 T/C (rs4991448) and exon 2 C/T (rs6446261) SNPs.

Gene/SNP Primer	Sequence (5' to 3')	Annealing Temperature (°C)	Amplicon size (bp)	Restriction Enzyme (Digested Products)
rs8179169				
GPX1 C/G FPG	TTGCGCCATGTGTGCTGCTCG	58	253	-
GPX1 C/G FPC	TTGCGCCATGTGTGCTGCTCC			
GPX1 C/G RP	AACTGGTTGCACGGGAAGCCG			
rs4991448				
GPX1 C/T F	GCGCCTGCTCGCCTCCCCTTAC	67	120	BsuRI (82 & 38 bp)
GPX1 C/T R	TTTCTCATGATAGTTTGGGTGTG			
rs6446261				
GPX1 C/T FPC	CCTTGAGACAGCAGGGC	65	279	-
GPX1 C/T FPT	CCTTGAGACAGCAGGGT			
GPX1 C/T R	CCAACTTCATGCTCTTCGAG			
HGH F	CCTTCCCAACCATTCCCTTA	61	428	-
HGH R	TCACGGATTTCTGTTGTGTTTC			
GPX1 expression F	GTTTGGGCATCAGGAGAACGCC	64	147	-
GPX1 expression R	AGGAAGGCGAAGAGAGGGTGC			
GAPDH expression F	ATCCCATCACCATCTTCCAGGA	65	122	-
GAPDH expression R	CAAATGAGCCCCAGCCTTCT			

2.2.3 Genotyping of *GPX1* exon1 G/C (rs8179169; Arg5Pro) polymorphism:

GPX1 exon1 G/C genotyping was done using amplification refractory mutation system-polymerase chain reaction (ARMS-PCR) method. DNA was amplified in two different PCR reactions with a generic antisense primer and one of the two allele specific sense primers (Table 2). To assess the success of PCR amplification in both the reactions, an internal control of 428 bp was amplified using a pair of primers designed from the nucleotide sequence of the human growth hormone (*HGH*) (Table 2). The reaction mixture of the total volume of 15 µL included 3 µL (100 ng) of genomic DNA, 4.9 µL nuclease-free H_2O, 1.5 µL 10x PCR buffer, 1.5 µL 10 mM dNTPs (SIGMA Chemical Co., St. Louis, Missouri, USA), 1 µL of 10 µM allele-specific and common primers (MWG Biotech, India), 1 µL of 10 µM control primers (*HGH*) and 0.1 µL (10U/µL) Taq Polymerase (Bangalore Genei, Bangalore, India). Amplification was performed using a

Mastercycler Gradient PCR (Eppendorf, Germany) according to the protocol: 95°C for 10 minute followed by 20 cycles of 95°C for 30 seconds, 61°C for 30 seconds, and 72°C for 30 seconds, then 20 cycles of 95°C for 30 seconds, 58°C for 30 seconds, and 72°C for 30 seconds. The amplified products were separated by electrophoresis on 2.5% agarose gel and stained with ethidium bromide. The gel was visualized under a UV transilluminator with a 100 base pair DNA ladder (Bioron, Ludwigshafen am Rhein, Germany) and photographed. Two amplicons were available for each sample (one each specific for G or C allele of the *GPX1* polymorphism).

2.2.4 Genotyping of *GPX1* exon1 T/C (rs4991448; Leu6Pro) polymorphism:

Polymerase chain reaction-restriction fragment length polymorphism (PCR-RFLP) was used to genotype T/C (rs4991448) polymorphism of *GPX1* gene (Figure 1). The primers used for genotyping are mentioned in Table 2. The reaction mixture of the total volume of 20 µL included 5 µL (100 ng) of genomic DNA, 10 µL nuclease-free H_2O, 2.0 µL 10x PCR buffer, 2 µL 2 mM dNTPs (SIGMA Chemical Co, St. Louis, Missouri, USA), 0.3 µL of 10 µM corresponding forward and reverse primers (Eurofins, Bangalore, India), and 0.3 µL (5U/µL) Taq Polymerase (Bangalore Genei, Bangalore, India). Amplification was performed using Mastercycler Gradient PCR (Eppendorf, Germany) according to the protocol: 95°C for 10 minutes followed by 35 cycles of 95°C for 30 seconds, 67°C for 30 seconds, and 72°C for 30 seconds. The amplified products were checked by electrophoresis on a 2.0% agarose gel stained with ethidium bromide. Restriction enzyme *Bsu*RI (Fermentas, Lithuania) was used for digestion of PCR amplicons of *GPX1* for genotyping of T/C (rs4991448) SNP (Table 2). Five µL of the amplified products were digested with 5 U of the restriction enzyme in a total reaction volume of 25 µL as per the manufacturer's instruction. The digested products with 50 bp DNA ladder (Bioron, Ludwigshafen am Rhein, Germany) were resolved on 3.5% agarose gels stained with ethidium bromide and visualized under UV trans-illuminator.

2.2.5 Genotyping of *GPX1* exon2 C/T (rs6446261; Ala194Thr) polymorphism:

GPX1 exon2 C/T (rs6446261) genotyping was done using ARMS-PCR method. DNA was amplified in two different PCR reactions with a generic antisense primer and one of the two allele specific sense primers (Table 2). The amplified products were separated by electrophoresis on 2.5% agarose gel and stained with ethidium bromide. The gel was visualized under a UV transilluminator with a 100 base pair DNA ladder (Bioron, Ludwigshafen am Rhein, Germany) and photographed. Two amplicons were available for each sample (one each specific for C or T allele of the *GPX1* polymorphism). More than 10% of the samples were randomly selected for confirmation and the results were 100% concordant (analysis of the chosen samples was repeated by two researchers independently).

2.2.6 Estimation of GPX enzyme activity:

Erythrocyte GPX activity was assayed according to the standard method of Paglia and Valentine (Paglia and Valentine, 1967), using GSH as a substrate. Briefly, 100 µL of 0.4 M phosphate buffer, 100 µL of GSH, 100 µL of Na-azide, 10 µL diluted sample (0.25 g% Hb) and make upto 400 µL using double distilled water into a vial. This reaction system was incubated at 37˚C for 5 min. After incubation 100 µL of 10 mM H_2O_2 was added and kept at 37˚C again for 3 min then 400 µL of precipitating reagent containing 0.2M glacial m-phosphoric acid, 5mM EDTA, 5mM NaCl was added to the existing system. Whole system was centrifuged at 3,000 rpm for 10 min. After centrifugation 600 µL of supernatant was pipetted into the cuvette and 600 µL of 0.4 M Na_2HPO_4 and 30 µL of 1mM DTNB were added. All chemicals used in assay were procured from SIGMA Chemical Co, St. Louis, Missouri, USA. The rate of GSH utilization was monitored spectrophotometrically at 412 nm. Blank was run for each sample. Activity of GPX was expressed as mmoles of GSH utilized/gHb/min.

2.2.7 Estimation of LPO levels:

Erythrocyte lipid peroxidation levels were estimated according to the standard procedure of Beuge and Aust (1978). Briefly, 1 ml of TBA reagent containing 6 mM thio-barbituric acid, 6 mM EDTA, 10% TCA and 2.5N HCl and 990 µL of diluted sample were taken into a vial, this system was incubated in boiling water bath for 20 min. After that it was centrifuged at 3,000 rpm for 10 min. Supernatant was pipetted into the cuvette. The rate of MDA formation was monitored spectrophotometrically at 532 nm. Blank was run for each sample. LPO level was expressed as nmoles of MDA formed/gHb/min. All chemicals used in assay were procured from SIGMA Chemical Co, Missouri, USA.

2.2.8 Determination of *GPX1* mRNA expression:

RNA extraction and cDNA synthesis

Total RNA from whole blood was isolated and purified using Ribopure™- blood Kit (Ambion inc. Texas, USA) following the manufacturer's protocol. RNA integrity was verified by 1.5% agarose gel electrophoresis, RNA yield and purity was determined spectrophotometrically at 260/280 nm. RNA was treated with DNase I (Ambion inc. Texas, USA) before cDNA synthesis to avoid DNA contamination. One microgram of total RNA was used to prepare cDNA. cDNA synthesis was performed using the Verso cDNA Kit (Thermo Fisher Scientific Inc., USA) according to the manufacturer's instructions in the Mastercycler Gradient PCR (Eppendorf, Germany).

Real-time PCR

The expression of *GPX1* and *GAPDH* transcripts were measured by real-time PCR using gene specific primers (Eurofins, Bangalore, India) as shown in Table 2. Expression of *GAPDH* gene was used as a reference. Real-time PCR was performed in duplicates in 20 μl volume using LightCycler®480 SYBR Green I Master (Roche Diagnostics GmbH, Mannheim, Germany) following the manufacturer's instructions and carried out in the Light Cycler 480 Real-Time PCR (Roche Diagnostics GmbH, Mannheim, Germany). The thermal cycling conditions included an initial activation step at 95°C for 10 min, followed by 45 cycles of denaturation, annealing and amplification (95°C for 10 s, 64°C for 20 s, 72°C for 20 s). The fluorescence data collection was performed during the extension step. At the end of the amplification phase a melt curve analysis was carried out to check the specificity of the products formed. The value of Cp was determined by the first cycle number at which fluorescence was greater than the set threshold value.

2.2.9 Statistical analyses:

Evaluation of the Hardy-Weinberg equilibrium (HWE) was performed for all three polymorphisms in patients and controls by comparing the observed and expected frequencies of the genotypes using chi-square analysis. The distribution of the genotypes and allele frequencies of polymorphisms in different groups, considering the major genotype / allele as a reference group and were compared using chi-square test with 2×2 contingency tables using Prism 4 software (Graph Pad Software, USA, 2003). A *p*-value <0.017 was considered as statistically significant due to Bonferroni's correction for multiple testing. Odds ratio (OR) with 95% confidence interval (CI) for disease susceptibility was also calculated. Haplotype analysis was carried out using http://analysis.bio-x.cn/myAnalysis.php (Shi *et al*., 2005). The LD coefficients D' and r^2-values for the pair of most common alleles at each site were estimated using the Haploview programe version 4.1 (Barrett *et al*., 2005). GPX1 activity, LPO levels, relative *GPX1* expression and genotype-phenotype correlation analysis was plotted and analyzed by nonparametric unpaired t-test using Prism 4 software (Graph Pad Software, USA, 2003). Statistical power of detection of association with the disease at 0.05 level of significance was determined by using G* Power software (Faul *et al*., 2007).

2.2.10 Bioinformatics analysis:

In silico prediction tools: SIFT (Kumar *et al*., 2009), PANTHER (Thomas *et al*., 2003), I-MUTATNT SUITE (Capriotti *et al*., 2008), POLYPHEN (Adzhubei *et al*., 2010), MUPRO (Cheng *et al*., 2006) were employed to predict the impact on the protein due to single amino acid variations. SNPs and GO (Capriotti *et al*., 2006) predicts the variation effect which might terminate into a disease like a trait. The crystal structure coordinates of the selenocysteine to glycine mutant of human GPX1 was downloaded from Protein Data Bank (PDB: 2F8A) (http://www.pdb.org). The observed mutation was done at sequence level and submitted for homology modeling to I-TASSER (Zhang, 2008; Roy *et al*., 2010, 2012). MD simulations were performed using the GROMACS version 4.5.4 (van der Spoel *et al*., 2010) and OPLS-AA/L all atom force field (Jorgensen *et al*., 1996).

Sorting Intolerant From Tolerant (SIFT)

SIFT predicts whether an amino acid substitution affects protein function. SIFT prediction is based on the degree of conservation of amino acid residues in sequence alignments derived from closely related sequences, collected through PSI-BLAST (Kumar *et al*., 2009).

I-MUTATNT

I-Mutant 2.0 is a Support Vector Machine -based web server for the prediction of protein stability changes upon single-site mutations. I-Mutant uses the data set derived from ProTherm (Bava *et al*., 2004) that is presently the most comprehensive database of experimental data on protein mutations. I-Mutant 2.0 predicts whether the protein mutation stabilizes or destabilizes the protein in 77% of the cases when the protein sequence is available (Capriotti *et al*., 2008).

Single Nucleotide Polymorphisms and Gene Ontology (SNPs & GO)

SNPs & GO is a web server for the prediction of human disease-related single point protein mutations from the protein sequence. SNPs & GO is based on support vector machines, that uses different pieces of information, including that derived from the Gene Ontology annotation to predict if a given mutation can be classified disease-related or not, scoring with accuracy=82% and Matthews correlation coefficient=0.63 (Capriotti *et al*., 2006).

Protein Analysis THrough Evolutionary Relationships (PANTHER)

PANTHER estimates the likelihood that a specific amino acid substitution in a protein will affect the protein's function, by calculating the subPSEC (substitution position-specific evolutionary conservation) score based on an alignment of evolutionarily related proteins (Thomas and Kejariwal, 2004) and statistics from hidden Markov models (Thomas *et al*., 2003; Mi *et al*., 2016).

Polymorphism Phenotyping v2 (PolyPhen-2)

PolyPhen-2 is an automatic tool for prediction of possible impact of an amino acid substitution on the structure and function of a human protein. This prediction is based on a number of features comprising the sequence, phylogenetic and structural information characterizing the substitution (Adzhubei *et al*., 2010). PolyPhen-2 predicts the functional significance of an allele replacement from sequence and structure-based features of the substitution site, by Naïve Bayes classifier using supervised machine-learning.

MUPRO

MUPRO uses support vector machines to predict protein stability changes for single amino acid mutations leveraging both sequence and structural information. The sign of the stability changes is considered, only when the predictive method achieves 84% accuracy. The prediction accuracy obtained using sequence alone is close to the accuracy obtained using tertiary structure information (Cheng *et al*., 2006).

2.2.10.1 *Homology modeling and structure validation*

Full length amino acid sequence of human GPX1 (accession number: P07203) was retrieved from Universal Protein Resource database (http:/www.uniprot.org/) with a predicted molecular mass of 22 kDa. Crystal structure coordinates of the selenocysteine to glycine mutant of human GPX1 was downloaded from Protein Data Bank (PDB: 2F8A) (http://www.pdb.org). The observed mutation was done at sequence level and submitted for homology modeling keeping PDB: 2F8A and bovine GPX PDB: 1GP1 as template to get precise model to I-TASSER (Zhang, 2008; Roy *et al*., 2010, 2012), which uses threading and simulation to generate 3D model. The best model was selected from I-TASSER which has c-score of higher value.

2.2.10.2 *Ttetramer generations of GPX1 wild and variant protein*

In analogy to bovine GPX1, human GPX1 exists as tetramer in cytoplasm (Epp *et al*., 1983; Meera Khan *et al*., 1984, Ren *et al*., 1997); we generated tetramer associations based on quaternary assembly of GPX1. The asymmetric unit consists of two subunits (one dimer) with the tetramer generated by a crystallographic 2-fold axis (Epp *et al*., 1983). The crystal structure coordinates of the selenocysteine to glycine mutant of human GPX1 exist in dimeric form so different combination and symmetry was taken in account for generation of tetrameric quaternary structure. A valid association was found after superimposing the generated model with already known assembly of human GPX1. Homology model with maximum number of residues in the favored regions and additional allowed regions in Ramachandran plot was selected for further investigations. Superimposition of the wild type, Arg5Pro and Leu6Pro homology models did not reveal any major structural differences among them except the N-terminal portion where the Arg5Pro, Leu6Pro variations are present.

2.2.10.3 *MD simulation of GPX1 wild type, Arg5Pro and Leu6Pro mutated models*

Molecular dynamics (MD) simulations were performed using the GROMACS version 4.5.4 (van der Spoel *et al*., 2010) and OPLS-AA/L all atom force field (Jorgensen *et al*., 1996). Simulation box was defined as cubic containing protein in the center of box and placed at least 1.0 nm away from the edge of box. Initial structures were solvated with SPC/E water molecule using spc216.gro, which is a generic equilibrated 3-point solvent model. The entire system contained 4 chains (A, B, C and D chain). Appropriate numbers of chloride ions were added to the box to neutralize the system. The solvated system was further energy minimized using steepest descent minimization method for up to maximum 50,000 steps so that the protein is relaxed with no steric clashes or inappropriate geometry. After energy minimization, MD simulations were performed for 100 ps at constant temperature (300 K) and pressure (1 atm) with periodic boundary conditions, Particle Mesh Ewald summation, and a 1-fs time step to heat and equilibrate the system. The time step was set to 2 fs for all simulations. Pressure was maintained at 1.0 bar and temperature was kept at 300 K according to the Berendsen integrating method (Berendsen *et al*., 2010). Electronic interactions were computed with the particle-mesh Ewald (PME) algorithm. This was followed by final production MD run of 1ns duration for each simulation. Coordinates were saved every 2ps. The relative binding energies were computed using the tool g energy module of ‘GROMACS 4.5.4'. The output files (.xvg) from was analyzed in XMGRACE program. The parameters analyzed were: energy variations (kinetic energy, potential energy and total energy), intra-molecular hydrogen bonds, inter-molecular hydrogen bonds with surrounding water molecules, radius of gyration, root mean square deviations (RMSD) of each amino acid residue, root mean square fluctuations (RMSF) of each amino acid residue, solvent accessible surface area, and hydrophobic and hydrophilic interactions. The obtained parameters for GPX1 wild, Arg5Pro and Leu6Pro mutants were compared.

2.3 RESULTS:

2.3.1 Analysis of association between *GPX1* exon1 G/C (rs8179169; Arg5Pro) polymorphism and susceptibility to vitiligo:

Only two genotypes identified in both patients and controls were: GG and GC for the G/C polymorphism (Figure 1A). 'GC' genotype was found to be significantly associated with vitiligo (p<0.0001, OR=1.726, CI=1.329-2.241; Table 3). In particular, minor allele 'C' was more frequent in the patients compared to controls (17.0% versus 11.0%, p=0.0002, OR=1.577, CI=1.242-2.002; Table 3). Analysis based on disease progression revealed that the increased frequency of the minor allele 'C' occurred predominantly in patients with AV (19.0% versus 11.0%, p<0.0001) compared to controls (Table 4). However, there was no significant difference between SV patients and controls (p=0.546) (Table 4). Interestingly, the 'GC' genotype was predominant in AV patients compared to SV (37.0% versus 26.0%, p=0.013) suggesting the important role of 'C' allele in disease progression. Further, analysis based on type of vitiligo revealed that the increased frequency of the minor allele 'C' occurred predominantly in patients with GV (20.0% versus 11.0%, p<0.0001) compared to controls (Table 5). However, there was no significant difference between LV patients and controls (p=0.578; Table 5). Interestingly, the 'GC' genotype was predominant in GV patients compared to LV (37.0% versus 25.0%, p=0.015) suggesting the important role of 'C' allele in GV. Moreover, analysis based on gender of vitiligo patients revealed that the increased frequency of the 'GC' genotype occurred predominantly in male patients (40.0% versus 29.0%, p=0.014) compared to female patients (Table 6). However, there was no significant difference in genotype and allele frequencies based on age of onset, family history of patients (data not shown). This study has 86.71% statistical power for the effect size 0.08 to detect the association of investigated polymorphisms at p<0.05 in patients and control population.

2.3.2 Analysis of association between *GPX*1 exon1 T/C (rs4991448; Leu6Pro) polymorphism and susceptibility to vitiligo:

Three genotypes were identified for T/C polymorphism (Figure 1B). 'TC' genotype was found to be significantly associated with vitiligo (p<0.0001, OR=1.766, CI=1.364-2.287)

(Table 3). In particular, the minor allele 'C' was more frequent in patients as compared to controls (21.0% versus 14.0%, $p<0.0001$, OR=1.593, CI=1.280-1.984) (Table 3). Analysis based on disease progression revealed that the increased frequency of minor allele 'C' occurred predominantly in AV patients (23.0% versus 14.0%, $p<0.0001$) compared to controls (Table 4). However, there was no significant difference between SV patients and controls ($p=0.641$; Table 4). Interestingly, the 'C' allele was predominant in AV patients compared to SV (23.0% versus 15.0%, $p=0.007$) suggesting the important role of minor allele 'C' in disease progression.

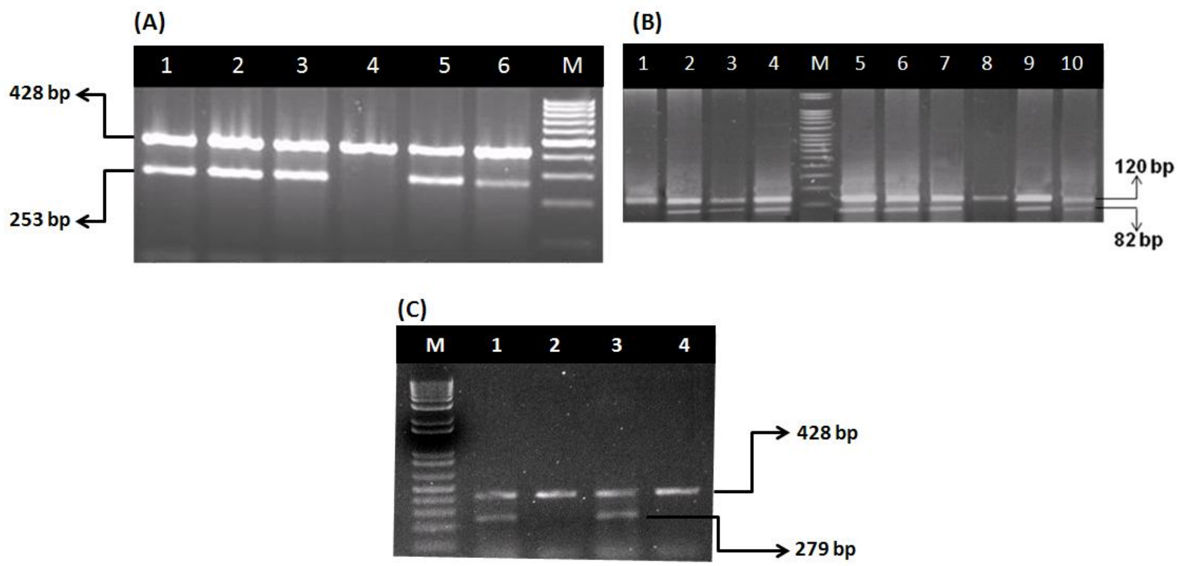

Figure 1. Genotyping of *GPX*1 gene polymorphisms: (A) ARMS-PCR analysis of *GPX1* G/C (rs8179169) polymorphism on 2.5 % agarose gel electrophoresis: lanes: 1, 2, 5 & 6 show heterozygous (GC) genotypes; lanes: 3 & 4 show homozygous (GG) genotypes; lane M shows 100 bp DNA ladder. **(B)** PCR-RFLP analysis of *GPX1* T/C (rs4991448) polymorphism on 3.5% agarose gel electrophoresis: lanes: 1 & 8 show homozygous (TT) genotypes; lanes: 2, 3, 4, 5, 6, 7, 9 & 10 show heterozygous (TC) genotypes; lane M shows 100 bp DNA ladder. **(C)** ARMS-PCR analysis of *GPX1* C/T (rs6446261) polymorphism on 2.5 % agarose gel electrophoresis: lanes: 1, 2, 3 and 4 show homozygous (CC) genotypes; lane M shows 100 bp DNA ladder.

Further, analysis based on type of vitiligo revealed that the increased frequency of the minor allele ‘C’ occurred predominantly in patients with GV (20.0% versus 14.0%, p=0.001) compared to controls (Table 5). Interestingly, the ‘C’ allele was predominant in LV patients compared to controls (24.0% versus 14.0%, p<0.0001) suggesting the important role of ‘C’ allele in LV. However, there was no significant difference between GV and LV patients (p=0.153; Table 5). Also, there was no significant difference in genotype and allele frequencies based on gender (Table 6), age of onset, and family history of patients (data not shown). This study has 86.71% statistical power for the effect size 0.08 to detect the association of investigated polymorphisms at p<0.05 in patients and control population.

2.3.3 Analysis of association between *GPX*1 exon2 C/T (rs6446261; Ala194Thr) polymorphism and susceptibility to vitiligo:

Only single genotype was observed i.e. CC for C/T SNP in both patient and control groups (Figure 1C). The observed allele frequencies of C and T were 1.00 and 0 respectively in controls and vitiligo patients (Table 3). Hence, we did not carry out further statistical analysis for this SNP.

2.3.4 Linkage disequilibrium (LD) and haplotype analyses:

The LD analysis revealed that the two polymorphisms (G/C Arg5Pro and T/C Leu6Pro) investigated in the *GPX1* were in moderate LD association (D’=0.675, r^2=0.352; Figure 2). A haplotype evaluation of the two polymorphic sites was performed and estimated frequencies of the haplotypes differed significantly between patients and controls (global p-value= $3.53e^{-009}$; Table 7). Interestingly, the frequency of susceptible haplotype ‘CC’ containing the minor alleles of both the polymorphisms were significantly higher in patients compared to controls (12.5% vs 8.8%; p=0.006) and increased the risk of vitiligo by 1.5-fold (OR=1.490; 95% CI= 1.117~1.986; Table 7). Also, the other two haplotypes: ‘CT’ and ‘GC’ were significantly increased in vitiligo patients as compared to controls (p=0.0004, p=5.09^{e-005}). The wild type haplotype ‘GT’ was more frequently observed in control group as compared to the patient group (83.5% vs 71.9%; p=4.34^{e-010}, Table 7).

Table 3. Association of *GPX1* exon 1 G/C (rs8179169), exon 1 T/C (rs4991448) and exon 2 C/T (rs6446261) polymorphisms in vitiligo patients from Gujarat.

SNP	Genotype or allele	Vitiligo Patients (Freq.)	Controls (Freq.)	*p* for HWE	*p* for Association	Odds ratio	CI (95%)
rs8179169 (G/C; Arg5Pro)	Genotype	(n = 521)	(n = 614)				
	GG	344 (0.66)	473 (0.77)	<0.0001 (P)	R	1	-
	GC	177 (0.34)	141 (0.23)		<0.0001[a]	1.726[a]	1.329-2.241[a]
	CC	00 (0.0)	00 (0.0)		-	-	-
	Allele			0.001 (C)			
	G	865 (0.83)	1087 (0.89)		R	1	-
	C	177 (0.17)	141 (0.11)		0.0002[b]	1.577[b]	1.242-2.002[b]
rs4991448 (T/C; Leu6Pro)	Genotype	(n = 521)	(n = 614)				
	TT	319 (0.61)	452 (0.74)	0.044 (P)	R	1	-
	TC	187 (0.36)	150 (0.24)		<0.0001[a]	1.766[a]	1.364-2.287[a]
	CC	15 (0.03)	12 (0.02)		0.142[a]	1.771[a]	0.818-3.836[a]
	Allele			0.913 (C)			
	T	825 (0.79)	1054 (0.86)		R	1	-
	C	217 (0.21)	174 (0.14)		<0.0001[b]	1.593[b]	1.280-1.984[b]
rs6446261 (C/T; Ala194Thr)	Genotype	(n = 521)	(n = 614)				
	CC	521 (1.0)	614 (1.0)	<0.0001 (P)			
	CT	0 (0.0)	0 (0.0)		1.0[a]	-	-
	TT	0 (0.0)	0 (0.0)				
	Allele			<0.0001 (C)			
	C	1042 (1.0)	1228 (1.0)		1.0[b]		
	T	0 (0.0)	0 (0.0)				

'n' represents number of samples, 'R' represents reference group, HWE refers to Hardy-Weinberg Equilibrium, CI refers to Confidence Interval, (P) refers to Patients and (C) refers to Controls, [a]Vitiligo Patients vs. Controls (genotype) using chi-squared test with 2 × 2 contingency table, [b]Vitiligo Patients vs. Controls (allele) using chi-squared test with 2 × 2 contingency table, Values are significant at $p \leq 0.017$ due to Bonferroni's correction.

Table 4. Association of *GPX1* exon 1 G/C (rs8179169) and exon 1 T/C (rs4991448) polymorphisms in patients with active and stable vitiligo from Gujarat.

SNP	Genotype or allele	Active Vitiligo (Freq.)	Stable Vitiligo (Freq.)	Controls (Freq.)	*p* for Association	Odds ratio	CI (95%)
rs8179169 (G/C; Arg5Pro)	Genotype	(n = 380)	(n = 141)	(n = 614)			
	GG	239 (0.63)	105 (0.74)	473 (0.77)	R	1	-
	GC	141 (0.37)	36 (0.26)	141 (0.23)	0.013[a] <0.0001[b] 0.516[c]	1.721[a] 1.979[b] 1.150[c]	1.12-2.65[a] 1.50-2.62[b] 0.75-1.76[c]
	CC	0 (0.0)	0 (0.0)	00 (0.0)	-	-	-
	Allele						
	G	619 (0.81)	246 (0.87)	1087 (0.89)	R	1	-
	C	141 (0.19)	36 (0.13)	141 (0.11)	0.027[a] <0.0001[b] 0.546[c]	1.557[a] 1.756[b] 1.128[c]	1.05-2.31[a] 1.36-2.26[b] 0.76-1.67[c]
rs4991448 (T/C; Leu6Pro)	Genotype	(n = 380)	(n = 141)	(n = 614)			
	TT	219 (0.58)	100 (0.71)	452 (0.74)	R	1	-
	TC	148 (0.39)	39 (0.28)	150 (0.24)	0.011[a] <0.0001[b] 0.444[c]	1.733[a] 2.036[b] 1.175[c]	1.13-2.65[a] 1.54-2.69[b] 0.78-1.78[c]
	CC	13 (0.03)	2 (0.01)	12 (0.02)	0.139[a] 0.044[b] 0.713[c]	2.968[a] 2.236[b] 0.753[c]	0.65-13.4[a] 1.00-4.98[b] 0.17-3.42[c]
	Allele						
	T	586 (0.77)	239 (0.85)	1054 (0.86)	R	1	-
	C	174 (0.23)	43 (0.15)	174 (0.14)	0.007[a] <0.0001[b] 0.641[c]	1.650[a] 1.799[b] 1.090[c]	1.14-2.38[a] 1.43-2.27[b] 0.76-1.57[c]

'n' represents number of samples, 'R' represents reference group, CI refers to Confidence Interval, [a]Active Vitiligo vs. Stable Vitiligo, [b]Active Vitiligo vs. Controls, [c]Stable Vitiligo vs. Controls, Values are significant at $p \leq 0.025$ due to Bonferroni's correction.

Table 5. Association of *GPX1* exon 1 G/C (rs8179169) and exon 1 T/C (rs4991448) polymorphisms in patients with generalized and localized vitiligo from Gujarat.

SNP	**Genotype or allele**	**Generalized Vitiligo (Freq.)**	**Localized Vitiligo (Freq.)**	**Controls (Freq.)**	***p* for Association**	**Odds ratio (OR)**	**CI (95%)**
	Genotype	(n = 387)	(n = 134)	(n = 614)			
rs8179169 (G/C; Arg5Pro)	GG	244 (0.63)	100 (0.75)	473 (0.77)	R	1	-
	GC	143 (0.37)	34 (0.25)	141 (0.23)	0.015[a] <0.0001[b] 0.551[c]	1.724[a] 1.966[b] 1.141[c]	1.11-2.68[a] 1.49-2.60[b] 0.74-1.76[c]
	CC	0 (0.0)	0 (0.0)	00 (0.0)	-	-	-
	Allele G	631 (0.82)	234 (0.87)	1087 (0.89)	R	1	-
	C	143 (0.20)	34 (0.13)	141 (0.11)	0.0296[a] <0.0001[b] 0.578[c]	1.560[a] 1.747[b] 1.128[c]	1.04-2.33[a] 1.36-2.25[b] 0.75-1.67[c]
	Genotype	(n = 387)	(n = 134)	(n = 614)			
rs4991448 (T/C; Leu6Pro)	TT	243 (0.63)	76 (0.57)	452 (0.74)	R	1	-
	TC	135 (0.35)	52 (0.39)	150 (0.24)	0.321[a] 0.0003[b] 0.0003[c]	0.812[a] 1.674[b] 2.062[c]	0.54-1.22[a] 1.26-2.22[b] 1.38-3.07[c]
	CC	9 (0.02)	6 (0.04)	12 (0.02)	0.155[a] 0.456[b] 0.027[c]	0.469[a] 1.39[b] 2.97[c]	0.16-1.36[a] 0.58-3.35[b] 1.08-8.16[c]
	Allele T	621 (0.80)	204 (0.76)	1054 (0.86)	R	1	-
	C	153 (0.20)	64 (0.24)	174 (0.14)	0.153[a] 0.001[b] <0.0001[c]	0.785[a] 1.49[b] 1.900[c]	0.56-1.09[a] 1.17-1.89[b] 1.38-2.63[c]

'n' represents number of samples, 'R' represents reference group, CI refers to Confidence Interval, [a]Generalized vitiligo vs. Localized vitiligo, [b]Generalized vitiligo vs. Controls, [c]Localized vitiligo vs. Controls, Values are significant at $p \leq 0.025$ due to Bonferroni's correction.

Table 6. Association of *GPX1* exon 1 G/C (rs8179169) and T/C (rs4991448) polymorphisms in male and female vitiligo patients from Gujarat.

SNP	Genotype or allele	Male (Freq.)	Female (Freq.)	*p* for Association	Odds ratio	CI (95%)
rs8179169 (G/C; Arg5Pro)	Genotype	(n = 235)	(n = 286)			
	GG	142 (0.60)	202 (0.71)	R	1	-
	GC	93 (0.40)	84 (0.29)	0.014[a]	1.575[a]	1.093-2.269[a]
	CC	00 (0.0)	00 (0.0)	-	-	-
	Allele					
	G	377 (0.80)	488 (0.85)	R	1	-
	C	93 (0.20)	84 (0.15)	0.029[b]	1.433[b]	1.036-1.982[b]
rs4991448 (T/C; Leu6Pro)	Genotype	(n = 235)	(n = 286)			
	TT	138 (0.59)	181 (0.63)	R	1	-
	TC	90 (0.38)	97 (0.34)	0.288[a]	1.217[a]	0.847-1.749[a]
	CC	7 (0.03)	8 (0.03)	0.795[a]	1.148[a]	0.406-3.242[a]
	Allele					
	T	366 (0.78)	459 (0.80)	R	1	-
	C	106 (0.22)	113 (0.20)	0.285[b]	1.176[b]	0.873-1.586[b]

'n' represents number of samples, 'R' represents reference group, CI refers to Confidence Interval, [a] Male vs. Female Patients (genotype) using chi-squared test with 2 × 2 contingency table, [b] Male vs. Female Patients (allele) using chi-squared test with 2 × 2 contingency table, Values are significant at p ≤ 0.025 due to Bonferroni's correction.

Table 7. Distribution of haplotypes frequencies for *GPX1* exon 1 G/C (rs8179169) and exon 1 T/C (rs4991448) polymorphisms in vitiligo patients and controls.

Haplotype [G/C rs8179169 and T/C rs4991448]	**Vitiligo Patients (Freq. %)**	**Controls (Freq. %)**	***p* for Association**	***p*(global)**	**Odds ratio (95% CI)**
G T	647 (0.719)	916 (0.835)	4.34^{e-010}	$3.53e^{-009}$	0.506 [0.408~0.628]
C C	113 (0.125)	96 (0.088)	0.006		1.490 [1.117~1.986]
C T	50 (0.056)	28 (0.025)	0.0004		2.287 [1.425~3.669]
G C	90 (0.100)	58 (0.053)	$5.09e^{-005}$		2.010 [1.426~2.832]

'CI' represents Confidence Interval, 'R' represents reference group, (Frequency <0.03 in both control & case has been dropped and was ignored in analysis).

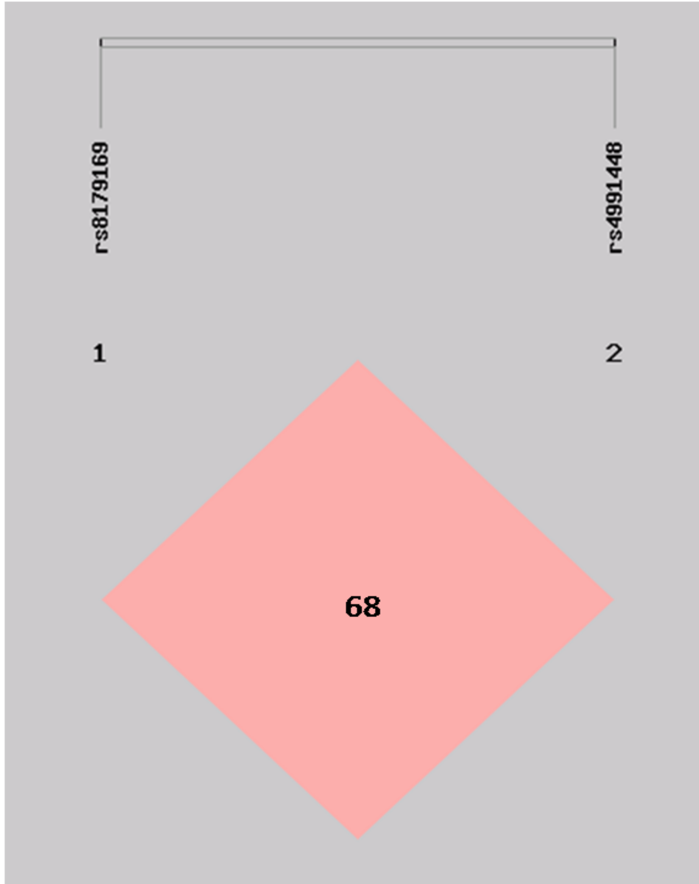

Figure 2. Linkage disequilibrium (LD) block: LD block with respect to *GPX1* exon 1 G/C (rs8179169) and T/C (rs4991448) polymorphisms in Gujarat population.

2.3.5 GPX1 activity in vitiligo patients

Comparison of the findings showed significant decrease in the GPX1 activity in vitiligo patients (n=521) as compared to controls (n=614) (p<0.0001; Figure 3A). Analysis showed ~1.93 fold change in the GPX1 activity in patients compared to controls. Further, male patients showed significant decrease in GPX1 activity compared to female patients (p=0.0358). In addition, we also checked the effect of GPX1 activity on progression of the disease and type of vitiligo. Interestingly, AV patients showed significant decrease in GPX1 activity compared to SV (p=0.007) suggesting the involvement of *GPX1* in disease progression. Moreover, GPX1 activity was significantly decreased in GV patients compared to LV (p<0.0001; Figure 3A).

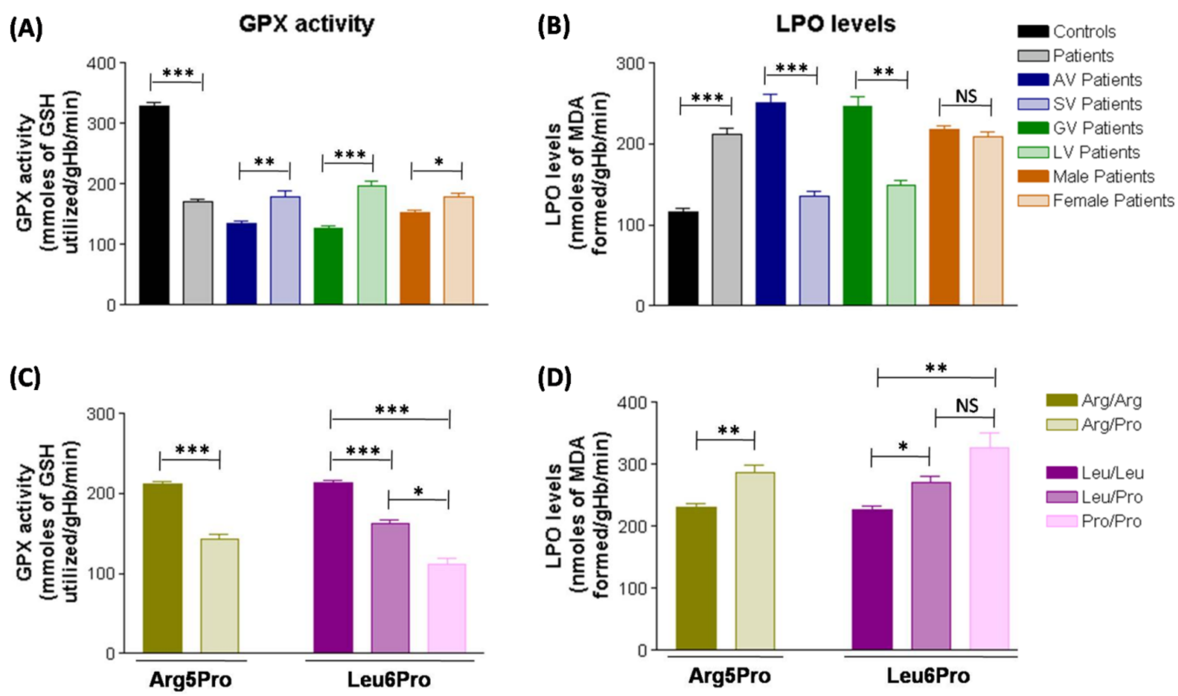

Figure 3. GPX1 activity, LPO levels and genotype-phenotype correlation analysis: (A) Vitiligo patients showed significantly decreased GPX1 activity as compared to controls (p<0.0001). AV patients showed significant decrease in GPX1 activity as compared to SV (p=0.007). GV patients showed significantly lower GPX1 activity as compared to LV (p<0.0001). Male patients showed significantly decreased GPX1 activity as compared to female patients (p=0.0358). **(B)** Patients showed significantly increased LPO levels as compared to controls (p<0.0001). AV patients showed significantly higher LPO levels as compared to SV (p<0.0001). GV patients showed significantly higher LPO levels as compared to LV (Mean ± SEM: 246.3 ± 20.58 vs 149.5 ± 11.16; p=0.001). Male/female patients did not show significant difference for LPO levels (p=0.562). **(C) GPX1 activity with respect to Arg5Pro and Leu6Pro polymorphisms:** Individuals with Arg/Pro genotype showed significant decrease in GPX1 activity (p<0.0001) as compared to individuals with Arg/Arg genotype. Individuals with Pro/Pro (p=0.0004) and Leu/Pro (p<0.0001) genotypes showed significant decrease in GPX1 activity as compared to Leu/Leu genotype. Also, individuals with Pro/Pro genotype showed decreased GPX1 activity as compared to Leu/Pro genotype (p=0.045). **(D) LPO levels with respect to Arg5Pro and Leu6Pro polymorphisms:** Individuals with Arg/Pro genotype showed significant increase in LPO levels as compared to Arg/Arg genotype (p=0.006). Individuals with Pro/Pro (p=0.003) and Leu/Pro (p=0.026) genotypes showed significant increase in LPO levels as compared to individuals with Leu/Leu genotype [*p<0.05; **p<0.01; ***p<0.001; NS = Non Significant (p>0.05)].

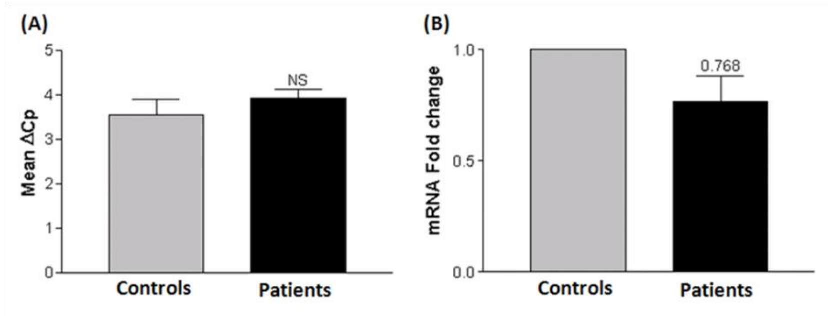

Figure 4: Relative gene expression of *GPX1* in patients with vitiligo and controls: (A) Comparison of the findings showed no significant difference in expression of *GPX1* transcript in 102 vitiligo patients than in 105 controls after normalization with *GAPDH* expression (Mean ΔCp ± SEM: 3.932 ± 0.2013 vs 3.551 ± 0.3594; p=0.378). **(B)** Expression of *GPX1* transcripts in vitiligo patients against controls showed 0.768 fold change as determined by the $2^{-\Delta\Delta Cp}$ method.

2.3.6 Relative gene expression of *GPX1* in vitiligo patients

Comparison of the findings showed no significant difference in expression of *GPX1* transcripts in 102 vitiligo patients than in 105 unaffected controls after normalization with *GAPDH* expression as suggested by mean ΔCp values (p=0.378; Figure 4). In addition, no significant difference was observed in *GPX1* expression in GV patients as compared to LV patients. Also, no significant difference was observed in *GPX1* expression in AV patients as compared to SV (data not shown).

2.3.7 LPO levels in vitiligo patients

Our findings showed significantly increased LPO levels in vitiligo patients (n=521) as compared to controls (n=614) (p<0.0001; Figure 3B). However, there was no significant difference in LPO levels between male patients and female patients (p=0.351). Analysis showed ~1.54 fold change increase in the LPO levels in patients compared to controls. Further, the LPO levels were analyzed with respect to progression of the disease and type of vitiligo. AV patients showed significant increased LPO levels compared to SV (p<0.0001) suggesting the involvement of oxidative stress in disease progression. Interestingly, LPO levels were also increased significantly in GV patients compared to LV (p=0.001; Figure 3B).

2.3.8 Genotype-phenotype correlation analysis:

The activity of GPX1 was analyzed with respect to G/C (Arg5Pro) genotypes (Figure 3C). Individuals with Arg/Pro (GC) genotype showed significantly decreased GPX1 activity (p<0.0001) compared to individuals with Arg/Arg (GG) genotype. In case of T/C (Leu6Pro) SNP, individuals with Pro/Pro (CC) genotype showed significantly decreased GPX1 activity (p=0.0004) compared to individuals with Leu/Leu (TT) genotype. Individuals with Leu/Pro (TC) genotype showed significantly decreased GPX1 activity (p<0.0001) compared to individuals with Leu/Leu (TT) genotype. Further, individuals with Pro/Pro (CC) genotype showed significantly decreased GPX1 activity (p=0.0449) compared to individuals with Leu/Pro (TC) genotype (Figure 3C).

Further, LPO levels were also analyzed with respect to G/C (Arg5Pro) genotypes (Figure 3D). Interestingly, individuals with Arg/Pro (GC) genotype showed significantly increased LPO levels (p=0.006) compared to individuals with Arg/Arg (GG) genotype. In case of T/C (Leu6Pro) SNP individuals with Pro/Pro (CC) genotype showed significantly increased LPO levels (p=0.023) compared to individuals with Leu/Leu (TT) genotype. Individuals with Leu/Pro (TC) genotype showed significantly increased LPO levels (p=0.026) compared to individuals with Leu/Leu (TT) genotype. However, individuals with Pro/Pro (CC) genotype did not show significant difference in LPO levels (p=0.328) compared to individuals with Leu/Pro (TC) genotype (Figure 3D).

2.3.9 Bioinformatics analysis:

2.3.9.1 *Sequence based in silico predictions*:

PANTHER tool showed GPX1 Arg5Pro, Leu6Pro and Ala194Thr variations to be deleterious for the GPX1 function, with highest score of -4.78994 and probability of ~86% for Leu6Pro variation (Table 8). POLYPHEN tool showed none of the substitutions affecting phenotype or having damaging effects on the function of GPX1 protein. However, the score of mutant Leu6Pro was little higher than other two variations indicating that, this variant behaves differently than others. I-MUTANT and MUPRO predictions revealed decreased stability of Leu6Pro and Ala194Thr variants compared to native structure, which will in turn affect the function of the protein. SNPs AND GO tool revealed Arg5Pro, Leu6Pro variants show disease like a trait. However, this tool could not return any output for Ala194Thr variation (Table 8).

Table 8. *In silico* prediction analysis for *GPX1* polymorphisms.

SNP	SIFT	PANTHER	SNPs and GO	POLYPHEN	I-MUTANT	I-MITANT Score	MUPRO
Arg5Pro	0.07	-3.980	Disease	0	Disease	0.07	Decrease
Leu6Pro	0.33	-4.789	Disease	0.021	Disease	-0.71	Decrease
Ala194Thr	0.56	-3.278	NA	0	Neutral	-2.15	Decrease

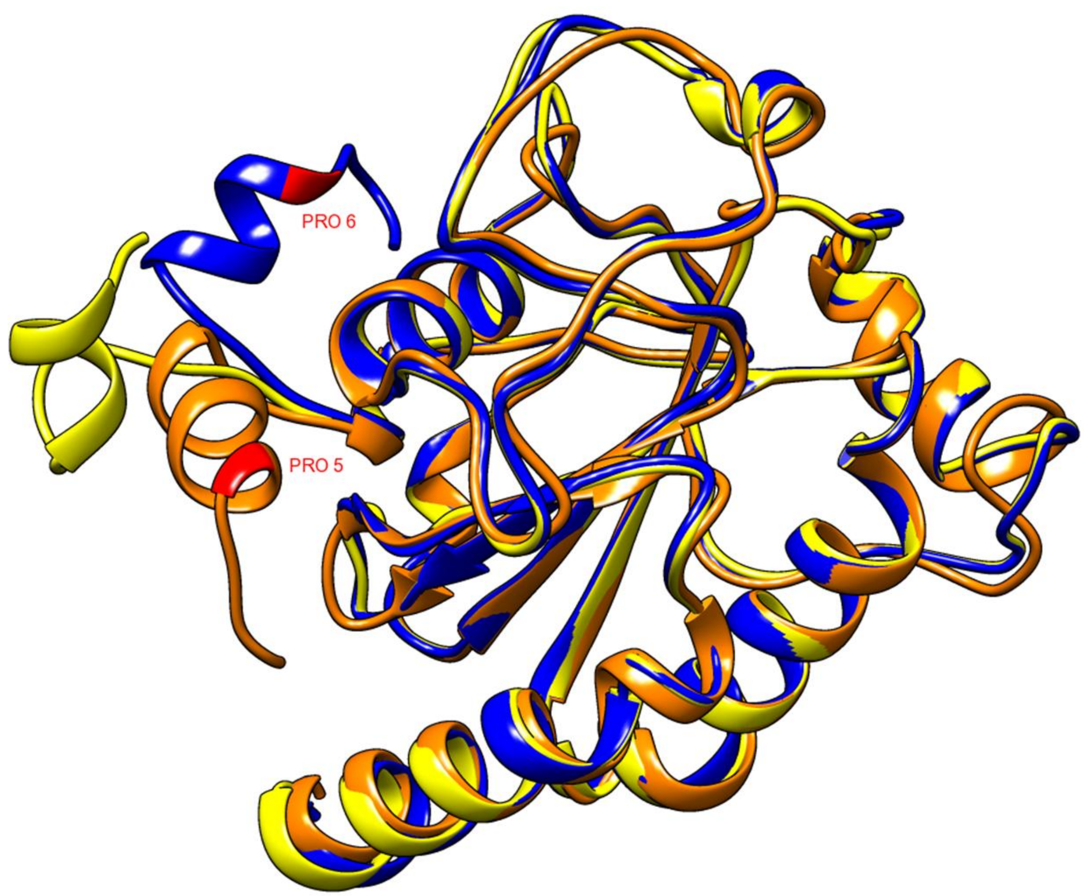

Figure 5: Structural superimposition of monomer GPX1 wild, Leu6Pro and Arg5Pro variants. GPX1 wild (yellow), Leu6Pro (blue) and Arg5Pro (orange); Gly119 and Ala120 shown to be in close proximity in Leu6Pro which is marked with red colour.

2.3.9.2 ***Structure based in silico predictions*:**

Molecular dynamics (MD) simulation was performed to investigated the structural differences as well as stability of GPX1 wild and Arg5Pro, Leu6Pro variants based on parameters such as energy variations (kinetic energy, potential energy and total energy), intra-molecular hydrogen bonds, inter-molecular hydrogen bonds with surrounding water molecules, radius of gyration (ROG), root mean square deviations (RMSD) and root mean square fluctuations (RMSF) of each amino acid residue, solvent accessible surface area and hydrophobic, hydrophilic interactions. Superimposition of the wild type, Arg5Pro and Leu6Pro homology models did not reveal any major structural differences among them except the N-terminal portion where the Arg5Pro, Leu6Pro variations are present (Figure 5).

Monomer MD simulation

RMSD of protein backbone was plotted as the time dependent function of MD simulations, to analyze the stability of predicted protein (Figure 6A) and fluctuations were recorded up to 0.34 nm, 0.21 nm and 0.24 nm for GPX1 wild type, Arg5Pro and Leu6Pro variants, respectively. Arg5Pro and Leu6Pro variants showed similar effect on the stability of GPX1 backbone which was clearly distinguishable from the wild type (Figure 6A), as the α-helix at N-terminal was bends towards the inner core of the protein in both the cases (Figure 6E). Variation in ROG values represents the variation in the compactness of the protein structure. ROG of GPX1 wild was initially fluctuated during first 500ps simulation and gradually it lowered down and attained stability during last 500ps simulation (Figure 6B). ROG of variant structures fluctuated alongside and much less deviation was found in ROG values of initial and later simulations. The mean deviation was 1.65 nm, 1.62 nm and 1.62 nm for GPX1 wild type, Arg5Pro and Leu6Pro variants respectively. Intra-molecular-H bonds formation during the simulations is shown in Figure 6C. Average intra-molecular-H bond in GPX1 wild type, Arg5Pro and Leu6Pro variants was found to be 130, 118 and 123 respectively. The standard deviation of GPX1 wild type, Arg5Pro and Leu6Pro variants was 4.96, 5.13 and 5.85 respectively, suggesting wild type is stable than variants based on intra-molecular-H bonds analysis. RMSF of all the residues was calculated during the 1ns simulation to locate the regions of higher flexibility in the protein (Figure 6D). RMSF of GPX1 wild was found to be more stable as compared to Arg5Pro and Leu6Pro variants. In particular, residues 22-32, 55-68, 92-124, 136-164 and 180-192 were less fluctuating in wild type compared to variants. In Leu6Pro, a significant fluctuation was found at 118-120 residues and similarly in Arg5Pro, a region from 180-190 residues was found to fluctuate significantly than the other two. In case of Leu6Pro variant, the N-terminal helix bended towards inner core of the protein and the fluctuating peak at residues 119 and 120 were in the close proximity (Figure 6E), since 'Pro' is known to introduce kinks into α-helix and thereby attains unusual helix formation.

Tetramer MD simulation

The stability of the quaternary structures was studied in similar ways as monomer simulation analysis. The deviation in RMSD for Arg5Pro was found to be less as compared to GPX1 wild and Leu6Pro. Mean ± standard deviation values of GPX1 wild, Arg5Pro and Leu6Pro variants were 0.29 ± 0.062 nm, 0.32 ± 0.069 nm, 0.19 ± 0.058 nm respectively, which suggested difference between GPX1 wild and Leu6Pro simulations (Figure 7A). In case of Leu6Pro, the average ROG was found to be less (3.06 nm) as compared to wild type (3.21 nm) (Figure 7B). Average intra-molecular-H bonds in GPX1 wild type, Arg5Pro and Leu6Pro variants were found to be 532, 387 and 343 respectively (Figure 7C) and this was consistent with the ROG graph. Residue wise fluctuation has been shown in Figure 7D for different chains.

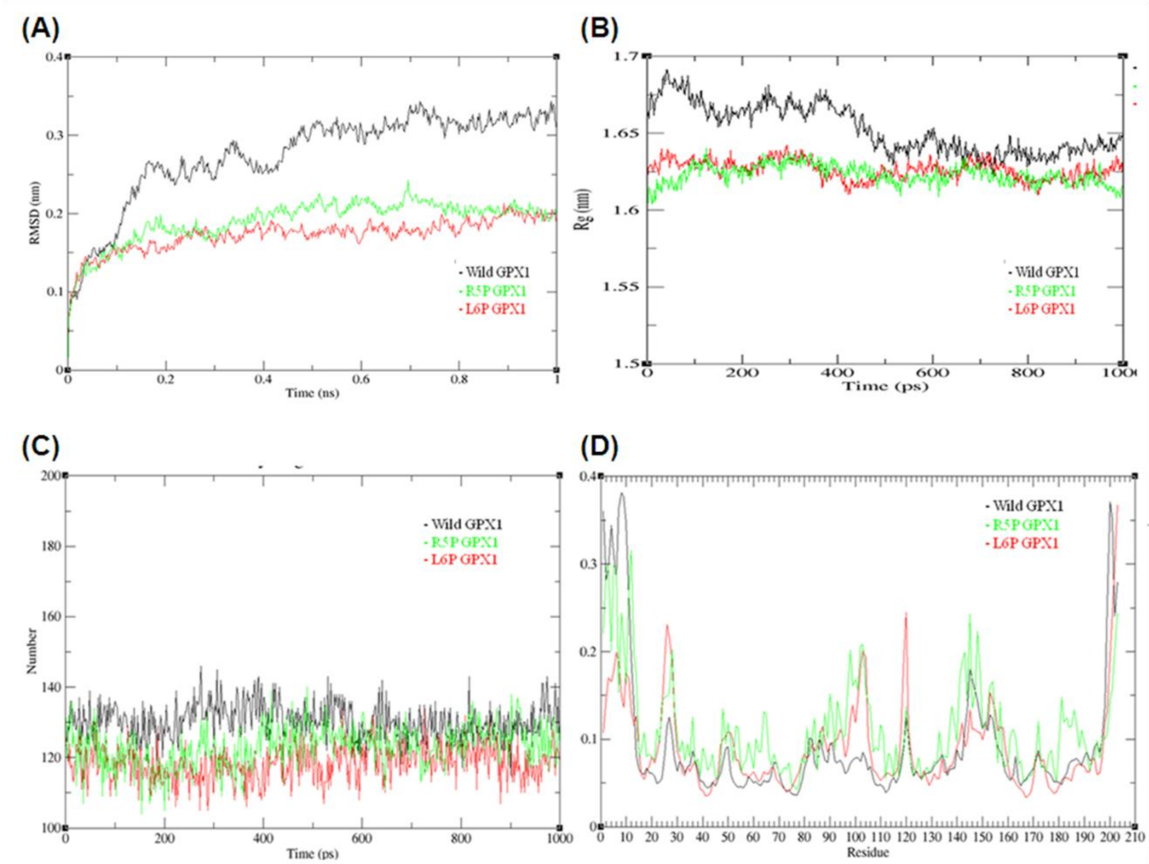

Figure 6: Monomer MD simulation: (A) Root mean square deviations (RMSD) of monomer forms of GPX1 wild, Arg5Pro (R5P) and Leu6Pro (L6P) variants. (B) Radius of Gyration (ROG) comparison of monomeric GPX1 wild, Arg5Pro and Leu6Pro variants. (C) Intra-molecular H bonds comparison of monomeric GPX1 wild, Arg5Pro and Leu6Pro variants. (D) Residue-wise root mean square fluctuations (RMSF) of monomeric GPX1 wild, Arg5Pro and Leu6Pro variants.

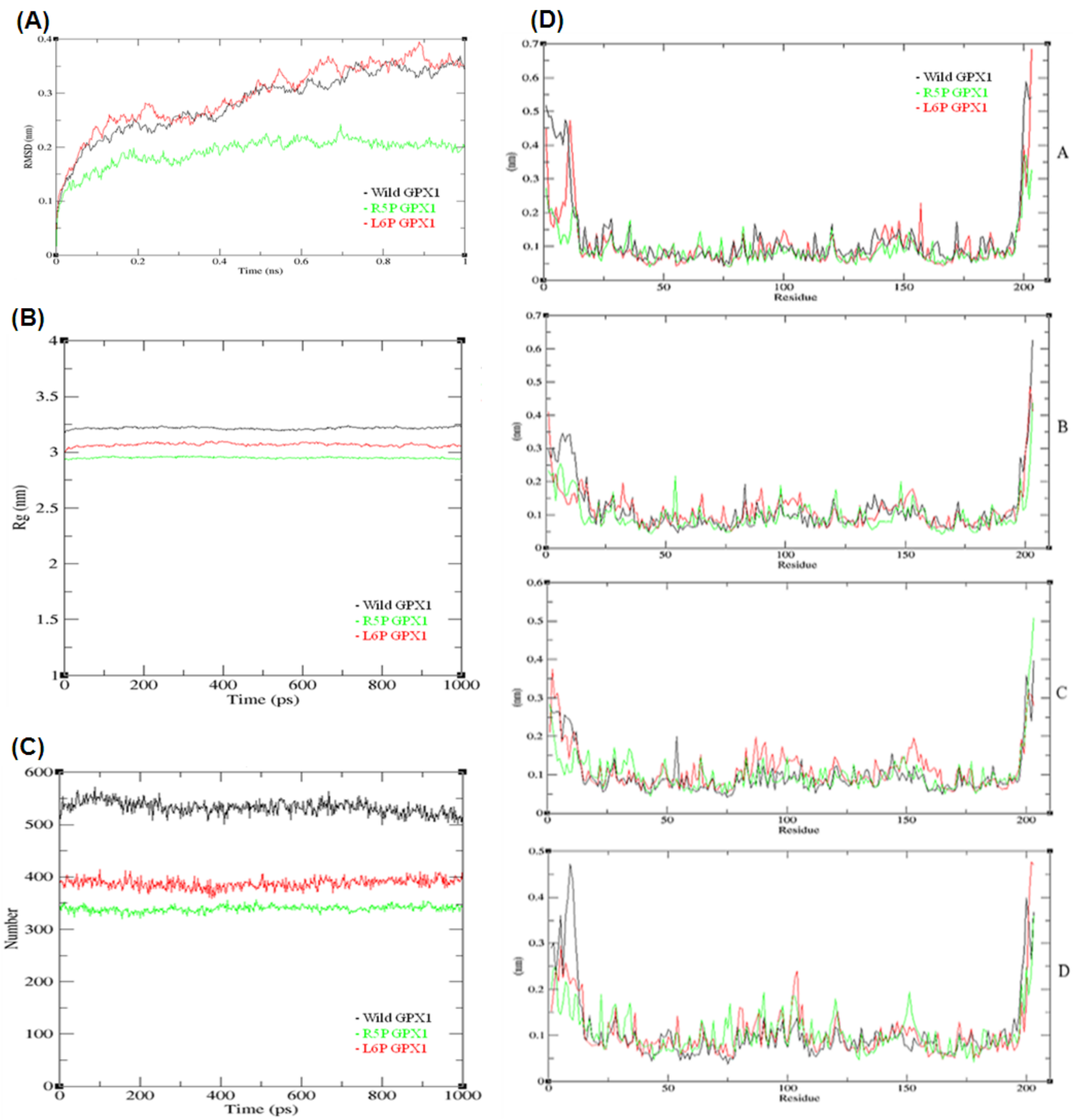

Figure 7: Tetramer MD simulation: (A) Change in RMSD of tetrameric GPX1 wild (black), Leu6Pro (red) and Arg5Pro (green). **(B)** Radius of Gyration (ROG) comparison GPX1 wild, Arg5Pro and Leu6Pro variants. **(C)** Intra-molecular H-bonds comparison of tetrameric of tetrameric GPX1 wild and Leu6Pro. **(D)** Residue-wise RMSF of tetrameric GPX1 wild, Arg5Pro and Leu6Pro.

2.4 DISCUSSION

There is strong evidence for the role of oxidative stress as a key factor in the onset and progression of vitiligo (Schallreuter *et al*., 1991; Maresca *et al*., 1997; Schallreuter *et al*., 1999; Laddha *et al*., 2013). ROS are frequently generated in epidermal cells following UV irradiation. Increased sensitivity of melanocytes from vitiligo patients to UVB induced cell death was attributed to their compromised capacity to cope with increased oxidative stress (Jimbow *et al*., 2001). Further evidence supports the exaggerated sensitivity of melanocytes from non-lesional vitiligo skin to chemical or physical oxidative stress (Maresca *et al*., 1997; Boissy and Manga, 2004). Vitiligo patients are known to have very high levels of H_2O_2 (1mM) in epidermis, concomitant with reduced activity of catalase (Schallreuter *et al*., 1991; Maresca *et al*., 1997; Schallreuter *et al*., 1999). Defective recycling of tetra-hydro-biopterin ($6BH_4$) has also been reported to generate ROS in vitiligo epidermis (Jiménez-Cervantes *et al*., 1998; Hornyak *et al*., 2000). The auto-cytotoxic premise suggests that melanocyte destruction could be related initially to an increased oxidative stress (Peinado *et al*., 1992; Tassabehji *et al*., 1994), with a subsequent induction of H_2O_2 accumulation in the epidermis of patients with active vitiligo (Bentley *et al*., 1994). The studies regarding GPX1 levels have given controversial results in vitiligo patients, though indicating an imbalance of antioxidants in vitiliginous skin as well as in blood (Passi *et al*., 1998; Beazley *et al*., 1999; Yildirim *et al*., 2003, 2004; Agrawal *et al*., 2004; Koca *et al*., 2004; Shajil and Begum, 2006; Ines *et al*., 2006; Shajil *et al*., 2007; Khan *et al*., 2009; Jain *et al*., 2011; Briganti *et al*., 2012). Reimann *et al*. (2012) have shown increased mRNA expression of *GPX1* in vitiligo lesions, compared to normal skin of patients with stable vitiligo, suggesting that increased *GPX1* expression might be involved in curbing the disease progression. Over-expression of *GPX*1 has been shown to increase the tolerance of MCF-7 cells to oxidative stress (Doroshow, 1995). GPX is reported to suppress apoptosis (Nomura *et al*., 1999; Gouaze *et al*., 2002). A number of studies including ours have reported the alteration in the systemic antioxidant pattern in vitiligo patients with reduced GPX, catalase and G6PD and increased SOD activities; which were correlated to higher LPO levels (Jiménez-Cervantes *et al*., 1998; Agrawal *et al*., 2004; Shajil and Begum, 2006; Laddha *et al*., 2013, 2014). In agreement to these, the present study also observed significant decrease in GPX1 activity and significant increase in LPO levels (Figure 3) in vitiligo patients as compared to controls, suggesting involvement of GPX1 in oxidative stress mediated pathogenesis of vitiligo. Although, vitiligo patients had lower *GPX1* expression as compared to controls (relative fold change = 0.768; Figure 4), it was statistically non-significant.

The present study focuses on instigation of genetic variants of *GPX1* which were significantly associated with decreased GPX1 activity in vitiligo patients (Table 8), hence might play a role in vitiligo susceptibility. Interestingly, for the first time we show the significant association of *GPX1* Arg5Pro and Leu6Pro polymorphisms with vitiligo susceptibility in Gujarat population (Table 3); however Ala194Thr polymorphism was found to be monogenic in population (Table 3) and seems to be highly conserved in population suggesting its functional importance. So far, there is only one report on *GPX1* Arg5Pro polymorphism in drug-induced liver injury cases, in which Lucena *et al*. (2010) did not find any genotypic variations, as all patients and controls were homozygous for the 'G' allele; whereas there is no report for *GPX1* Leu6Pro and Ala194Thr SNPs. The frequency of susceptible haplotype 'CC' was significantly high in vitiligo patients as compared to controls (p=0.006, OR=1.490, CI=1.117~1.986), indicating 1.49 fold risk for vitiligo susceptibility in individuals with 'CC' haplotype (Table 7). Interestingly, the genotype-phenotype correlation analysis for both *GPX1* Arg5Pro and Leu6Pro polymorphisms revealed positive correlation between decreased GPX1 activity (Figure 3C) and significant increase in LPO levels (Figure 3D) in individuals with Arg/Pro, Leu/Pro and Pro/Pro genotypes as compared to ancestral genotypes, indicating that 'Pro' allele might be involved in the decreased activity of GPX1.

In addition, both GV and AV patients showed significantly decreased GPX1 activity (Figure 3A) and increased LPO levels (Figure 3B) as compared to LV and SV respectively, indicating the involvement of GPX1 in disease progression as well. Male patients showed decreased GPX1 activity as compared to female patients (Figure 3A); however, no difference was observed in LPO levels (Figure 3B). Male patients showed significant association with Arg5Pro polymorphism as compared to female patients (Table 6). Interestingly, the 'C (Pro)' allele of Arg5Pro polymorphism was found to be predominant in active-generalized vitiligo patients; whereas in case of Leu6Pro polymorphism, the ‘C (Pro)’ allele was found to be predominant in active-localized vitiligo patients (Table 4 & 5), which signifies both polymorphisms modulate the disease progression in different fashion.

Nevertheless, the exact functional consequences of these polymorphic variants are unknown. The complexity of GPX1 activity regulation raised several interesting possibilities for studying how the sequence variations in *GPX1* might impact antioxidant system function. The current study could not perform the *in vitro* functional study of the SNPs, which might be considered as a limitation of the present study. Therefore, we investigated the structural and functional impacts of these polymorphisms on GPX1 through *in silico* approach using bioinformatics tools. *GPX1* is mapped on chromosome 3p21.3 and consist of about 180 ± 30 amino acids. In analogy to bovine GPX1, human GPX1 exists as tetramer in cytoplasm (Epp *et al*., 1983; Meera Khan *et al*., 1984; Ren *et al*., 1997). The asymmetric unit consists of two subunits (one dimer) with the tetramer generated by a crystallographic 2-fold axis (Epp *et al*., 1983). The monomer shows the typical structural motif of the thioredoxin fold consisting mainly of a central β-sheet with several flanking α-helices and an N-terminal short anti-parallel β-sheet packed forming a three-layered structure (Martin, 1995). A central helix (Glu88-Val97) and several loop regions contribute to inter-dimer interactions with main-chain and side-chain contacts provided by residues Tyr96, Glu89, Arg98, Asn84, Gly80 and His81 (Kavanagh *et al*., 2005, 2007). The active site selenocysteine residue ‘SeCys47’ is located in a shallow pocket at the interface between two monomer subunits, which is found at the N-terminal end of helix α1, and is found in the vicinity of the C-terminal end of strands β1 and β2 forming a β/α/β substructure which might constitute the substrate binding region (Epp *et al*., 1983). The dipole moment of helix α1 is presumably enhancing the nucleophilicity of the SeCys residue in its selenolate state (Epp *et al*., 1983). The SeCys residue is likely hydrogen bonded to residues Gln82 and Trp160 (Kavanagh *et al*., 2005, 2007).

In the present study, monomer GPX1 MD simulation analysis (analyze the stability of predicted protein) revealed the effect of Arg5Pro and Leu6Pro variations on the GPX1 backbone stability (Figure 6A). ‘Pro’ is often found in very tight turns (i.e. where the polypeptide chain must change the direction) in secondary structure of protein.

Interestingly, the position of the Arg5Pro and Leu6Pro residues also fell in α-helix and the helix at N-terminal bended towards the inner core of the protein in both the cases (Figure 6E). Variation in ROG values (represents the variation in the compactness of the protein structure) also showed that initially the GPX1 wild structure tends to grow but gradually the protein became compact to attain the stability (Figure 6B). Further, intra-molecular H-bonds in Arg5Pro and Leu6Pro were found to be lesser compared to wild type (Figure 6C), which might be due to the presence of variant 'Pro' residue (as it has no donor atom for recipient hydrogen), suggesting wild type is more stable than variants. Furthermore, RMSF which locates the regions of higher flexibility in the protein showed that GPX1 wild is more stable than variants (Figure 6D).

Moreover, tetramer MD simulation analysis showed similar results for Arg5Pro and Leu6Pro variants of GPX1 (Figure 7). Interestingly, in case of Leu6Pro the average ROG was lesser compared to wild type, indicating that protein has compacted during the simulations which might affects the binding to GSH substrate leading to altered GPX1 activity. For the first time, our study demonstrates the genotype-phenotype correlation of *GPX1* variants in vitiligo; however, further investigations are needed to elaborate the mechanistic insights that might reveal functional consequences of *GPX1* variants in vitiligo. These findings suggest that GPX1 could trigger or exaggerate the oxidative stress in vitiligo, leading to destruction of melanocytes.

Overall, the present study for the first time confirms the genetic association of vitiligo with variations in *GPX1*, which contains at least two independent risk signals, one tagged by the G/C (Arg5Pro) SNP and another tagged by the T/C (Leu6Pro) SNP. The study also emphasizes the influence of these SNPs on decreased GPX1 activity in patients which was also supported by our simulation studies on the mutation involved, suggests the crucial role of genetic factors and oxidative stress in vitiligo pathogenesis.

2.5 REFERENCES

Adzhubei IA, Schmidt S, Peshkin L, *et al*. (2010) A method and server for predicting damaging missense mutations. Nat Methods. 7: 248–249.

Agrawal D, Shajil EM, Marfatia YS, *et al*. (2004) Study on the antioxidant status of vitiligo patients of different age groups in Baroda. Pigment Cell Res. 17: 289-294.

Barrett JC, Fry B, Maller J, *et al*. (2005 Haploview: analysis and visualization of LD and haplotype maps. Bioinformatics. 21: 263-265.

Beazley WD, Gaze D, Panke A, *et al*. (1999) Serum selenium levels and blood glutathione peroxidase activities in vitiligo. Br J Dermatol. 141: 301-303.

Bava KA, Gromiha MM, Uedaira H, *et al*. (2004) ProTherm, version 4.0: thermodynamic database for proteins and mutants. Nucleic Acids Res 32: 120-121.

Bentley NJ, Eisen T, Goding CR. (1994) Melanocyte-specific expression of the human tyrosinase promoter: Activation by the microphthalmia gene product and role of the initiator. Mol Cell Biol. 14: 7996–8006.

Berendsen HJC, Postma JPM, van Gunsteren WF, *et al*. (1984) Molecular-Dynamics with Coupling to an External Bath. Journal of Chemical Physics. 81: 3684–3690.

Beuge JA, Aust SD. Microsomal lipid peroxidation. Methods in Enzymol. 52:302-310.

Boissy RE, Manga P. (2004) On the etiology of contact/occupational vitiligo. Pigment Cell Res. 17: 208-214.

Briganti S, Caron-Schreinemachers AL, Picardo M, *et al*. (2012) Anti-oxidant defence mechanism in vitiliginous skin increases with skin type. J Eur Acad Dermatol Venereol. 26: 1212-1219.

Capriotti E, Calabrese R, Casadio R. (2006) Predicting the insurgence of human genetic diseases associated to single point protein mutations with support vector machines and evolutionary information. Bioinformatics. 22: 2729–2734.

Capriotti E, Fariselli P, Rossi I, *et al*. (2008) A three-state prediction of single point mutations on protein stability changes. BMC Bioinformatics. 9: S2-S6.

Chen J, Cao Q, Qin C, *et al*. (2011) GPX-1 polymorphism (rs1050450) contributes to tumor susceptibility: evidence from meta-analysis. J Cancer Res Clin Oncol. 137: 1553-1561.

Cheng J, Randall A, Baldi P. (2006) Prediction of protein stability changes for single-site mutations using support vector machines. Proteins. 62: 1125–1132.

Doroshow JH. (1995) Glutathione peroxidase and oxidative stress. Toxicology Letters. 82: 395–398.

El-Far MA, Bakr MA, Farahat SE, *et al*. (2005) Glutathione peroxidase activity in patients with renal disorders. Clin Exp Nephrol. 9:127-131.

Epp O, Ladenstein R, Wendel A. (1983) The refined structure of the selenoenzyme glutathione peroxidase at 0.2-nm resolution. Eur J Biochem. 133: 51-69.

Ezzedine K, Lim HW, Suzuki T *et al*. (2012) Vitiligo Global Issue Consensus Conference Panelists. Revised classification/nomenclature of vitiligo and related issues: the Vitiligo Global Issues Consensus Conference. Pigment Cell Melanoma Res. 25: E1-E13.

Falabella R, Arrunategui A, Barona MI, *et al*. (1995) The minigrafting test for vitiligo: detection of stable lesions for melanocyte transplantation. J Am Acad Dermatol. 32: 228–232.

Faul F, Erdfelder E, Lang AG, *et al*. (2007) G*Power 3: A flexible statistical power analysis program for the social, behavioral, and biomedical sciences. Behav Res Methods.39: 175-191.

Gouaze V, Andrieu-Abadie N, Cuvillier O, *et al*. (2002) Glutathione peroxidase-1 protects from CD95-induced apoptosis. J Biol Chem. 277: 42867-42874.

Hamanishi T, Furuta H, Kato H, *et al*. (2004) Functional variants in the glutathione peroxidase-1 (GPX-1) gene are associated with increased intima-media thickness of carotid arteries and risk of macrovascular diseases in japanese type 2 diabetic patients. Diabetes. 53: 2455-2460.

Handy DE, Lubos E, Yang Y, *et al*. (2009) Glutathione peroxidase-1 regulates mitochondrial function to modulate redox-dependent cellular responses. J Biol Chem. 284: 11913-11921.

Hasse S, Gibbons NCJ, Rokos H, *et al*. (2004) Perturbed 6-tetrahydrobiopterin recycling via decreased dihydropteridine reductase in Vitiligo: more evidence for H_2O_2 stress. J Invest Dermatol. 122: 307-313.

Hornyak T, Hayes D, Ziff E. (2000) Cell-density-dependent regulation of expression and glycosylation od dopachrome tautomerase/tyrosinase-related protein-2. J Invest Dermatol. 115: 106–112.

Hu YJ and Diamond AM. (2003) Role of glutathione peroxidase 1 in breast cancer: Loss of heterozygosity and allelic differences in the response to selenium. Cancer Res. 63: 3347-3351.

Ines D, Sonia B, Riadh BM, *et al*. (2006) A comparative study of oxidant-antioxidant status in stable and active vitiligo patients. Arch Dermatol Res. 298: 147-152.

Jain A, Mal J, Mehndiratta V, *et al*. (2011) Study of oxidative stress in vitiligo. Indian J Clin Biochem. 26: 78–81.

Jalel A, Hédi Hamdaoui M. (2009) Study of Total Antioxidant Status and Glutathione Peroxidase Activity in Tunisian Vitiligo Patients. Indian J Dermatol. 54: 13–16.

Jimbow K, Chen H, Park JS, *et al*. (2001) Increased sensitivity of melanocytes to oxidative stress and abnormal expression of tyrosinase-related protein in vitiligo. Br J Dermatol. 144: 55-65.

Jiménez-Cervantes C, Martínez-Esparza M, Solano F, *et al*. (1998) Molecular interactions within the melanogenic complex: Formation of heterodimers of tyrosinase and TRP1 from B16 mouse melanoma. Biochem Biophys Res Commun. 253: 761–767.

Jorgensen WL, Maxwell DS, Tirado-Rives J. (1996) Development and Testing of the OPLS All-Atom Force Field on Conformational Energetics and Properties of Organic Liquids. J Am Chem Soc .118: 11225-11236.

Kavanagh KL, Johansson C, Smee C, *et al*. Crystal structure of the selenocysteine to glycine mutant of human glutathione peroxidase 1. 2005: DOI:10.2210/pdb2f8a/pdb.

Kavanagh KL, Johansson C, Smee C, *et al*. GPX1 - Human glutathione peroxidase 1. 2007: URL: http://www.thesgc.org/sites/default/files/activeISee/GPX1A_2f8a_v4_351m/GPX1A_2f8a_v4_351m_index.html.

Khan R, Satyam A, Gupta S, *et al*. (2009) Circulatory levels of antioxidants and lipid peroxidation in Indian patients with generalized and localized vitiligo. Arch Dermatol Res. 301: 731–737.

Koca R, Armutcu H, Altinyazar HC, *et al*. (2004) Oxidant antioxidant enzymes and lipid peroxidation in generalized vitiligo. Clin and Exp Dermatol. 29: 406-409.

Kumar P, Henikoff S, Ng PC. (2009) Predicting the effects of coding non-synonymous variants on protein function using the SIFT algorithm. Nat Protoc. 4: 1073-1081.

Laddha NC, Dwivedi M, Gani AR, *et al*. (2013) Involvement of Superoxide Dismutase Isoenzymes and their genetic variants in progression and higher susceptibility towards Vitiligo. Free Rad Biol & Med. 65: 1110-1125.

Laddha NC, Dwivedi M, Mansuri MS, *et al*. (2014) Role of Oxidative Stress and Autoimmunity in Onset and Progression of Vitiligo. Exp Dermatol. 23: 345-368.

Laddha NC, Dwivedi M, Mansuri MS, *et al*. (2013) Vitiligo: interplay between oxidative stress and immune system. Exp Dermatol. 22: 245-250.

Lucena MI, García-Martín E, Andrade RJ, *et al*. (2010) Mitochondrial superoxide dismutase and glutathione peroxidase in idiosyncratic drug-induced liver injury. Hepatology. 52: 303-312.

Majumder PP, Nordlund JJ, Nath SK. (1993) Pattern of familial aggregation of vitiligo. Arch Dermatol. 129: 994-998.

Maresca V, Roccella M, Roccella F, *et al*. (1997) Increased sensitivity to peroxidative agents as a possible pathogenic factor of melanocytes damage in vitiligo. J Invest Dermatol. 109: 310–313.

Martin JL. (1995) Thioredoxin--a fold for all reasons. Structure. 3: 245-250.

Meera Khan P, Verma C, Wijnen LM, *et al*. (1984) Red cell glutathione peroxidase (GPX1) variation in Afro-Jamaican, Asiatic Indian, and Dutch populations. Is the GPX1*2 allele of "Thomas" variant an African marker? Hum Genet. 66: 352-355.

Mi H, Poudel S, Muruganujan A, *et al*. (2016) PANTHER version 10: expanded protein families and functions, and analysis tools. Nucleic Acids Res. 44: D336-42.

Nath SK, Majumder PP, Nordlund JJ. (1994) Genetic epidemiology of vitiligo: multilocus recessivity cross-validated. Am J Hum Genet. 55: 981-990.

Nomura K, Imai H, Koumura T, *et al*. (1999) Mitochondrial phospholipid hydroperoxide glutathione peroxidase suppresses apoptosis mediated by a mitochondrial death pathway. J Biol Chem. 274: 29294-29302.

Ortonne JP, Bose SK. (1993) Vitiligo: Where do we stand? Pigment Cell Res. 8: 61-72.

Paglia DE, Valentine WN. (1967) Studies on quantitative and qualitative characterization of erythrocyte glutathione peroxidase. J Lab Clin Med. 70: 158-169.

Papp LV, Lu J, Holmgren A, *et al*. (2007) From selenium to selenoproteins: synthesis, identity, and their role in human health. Antioxid Redox Signal. 9: 775-806.

Passi S, Grandinetti M, Maggio F, *et al*. (1998) Epidermal oxidative stress in vitiligo. Pigment Cell Res. 11: 81–85.

Peinado P, Martínez-Liarte JH, del Marmol V, *et al*. (1992) Glutathione depletion in mouse melanoma cells increases their sensitivity to oxidative lysis. Cancer J. 5: 348–353.

Picardo M, Passi S, Morrone A, *et al*. (1994) Antioxidant status in the blood of patients with active vitiligo. Pigment Cell Res. 2: 110-115.

Ratnasinghe D, Tangrea JA, Andersen MR, *et al*. (2000) Glutathione peroxidase codon 198 polymorphism variant increases lung cancer risk. Cancer Res. 60: 6381-6383.

Reimann E, Kingo K, Karelson M, *et al*. (2012) Expression profile of genes associated with the dopamine pathway in vitiligo skin biopsies and blood sera. Dermatology. 224: 168-176.

Ren B, Huang W, Akesson B, *et al*. (1997) The crystal structure of seleno-glutathione peroxidase from human plasma at 2.9 A resolution. J Mol Biol. 268: 869-885.

Rotruck JT, Pope AL, Ganther HE, *et al*. (1973) Selenium: biochemical role as a component of glutathione peroxidase. Science. 179: 588-590.

Roy A, Kucukural A, Zhang Y. (2010) I-TASSER: a unified platform for automated protein structure and function prediction. Nature Protocols. 5: 725-38.

Roy A, Yang J, Zhang Y. (2012) COFACTOR: An accurate comparative algorithm for structure-based protein function annotation. Nucleic Acids Research. 40: W471-W477.

Schallreuter KU, Moore J, Wood JM, *et al*. (1999) In vivo and in vitro evidence for hydrogen peroxide (H_2O_2) accumulation in the epidermis of patients with vitiligo and its successful removal by a UVB-activated pseudocatalase. J Invest Dermatol Symp Proc. 4: 91–96.

Schallreuter KU, Wood JM, Berger J. (1991) Low catalase levels in the epidermis of patients with vitiligo. J Invest Dermatol. 97: 1081–1085.

Shajil EM, Begum R. (2006) Antioxidant status of segmental and non-segmental vitiligo. Pigment Cell Res. 19: 179–180.

Shajil EM, Laddha NC, Chatterjee S, *et al*.(2007) Association of catalase T/C exon 9 and glutathione peroxidase codon 200 polymorphisms in relation to their activities and oxidative stress with vitiligo susceptibility in Gujarat population. Pigment Cell Res. 20: 405-407.

Shi YY, He L. (2005) SHEsis, a powerful software platform for analyses of linkage disequilibrium, haplotype construction, and genetic association at polymorphism loci. Cell Res. 15: 97-98.

Sun X, Xu A, Wei X, *et al*. (2006) Genetic epidemiology of vitiligo: a study of 815 probands and their families from south China. Int J Dermatol. 45: 1176-1181.

Tassabehji M, Newton VE, Read AP. (1994) Waardenburg syndrome type 2 caused by mutations in the human microphthalmia (MITF) gene. Nat Genet. 8: 251–255.

Thomas PD and Kejariwal A. (2004) Coding single-nucleotide polymorphisms associated with complex vs. Mendelian disease: Evolutionary evidence for differences e. PNAS. 101: 15398-15403.

Thomas PD, Campbell MJ, Kejariwal A, *et al*. (2003) PANTHER: a library of protein families and subfamilies indexed by function. Genome Res. 3: 2129-2141.

van der Spoel D, Lindahl E, Hess B, *et al*. (2010) Gromacs User Manual version 4.5.4, www.gromacs.org

Wei HL, Pei JR, Jiang CX, *et al*. (2011) Analysis of glutathione peroxidase 1 gene polymorphism and Keshan disease in Heilongjiang Province, China. Genet Mol Res.10: 2996-3001.

Yildirim M, Baysal V, Inaloz HS, *et al*. (2003) The role of oxidants and antioxidants in generalized vitiligo. J Dermatol. 2: 104-108.

Yildirim M, Baysal V, Inaloz HS, *et al*. (2004) The role of oxidants and antioxidants in generalized vitiligo at tissue level. J Eur Acad Dermatol Venereol. 18: 683–686.

Zailaie MZ. (2005) Effect of prolonged low-dose oral aspirin on the oxidative status of peripheral blood mononuclear cells of active vitiligo. Indian J Dermatol. 50: 9-16.

Zhang Y. (2008) I-TASSER server for protein 3D structure prediction. BMC Bioinformatics. 9: 40.

Zotova EV, Savost'ianov KV, Chistiakov DA, *et al*. (2004) Search for the association of polymorphic markers for genes coding for antioxidant defense enzymes, with development of diabetic polyneuropathies in patients with type 1 diabetes mellitus. Mol Biol (Mosk). 38: 244-249.